Journal of Applied Pharmaceutical Science Vol. 8(05), pp 119-128, May, 2018
Available online at http://www.japsonline.com
DOI: 10.7324/JAPS.2018.8516
ISSN 2231-3354

Biosynthesis Physico-Chemical Optimization of Gold Nanoparticles as Anti-Cancer and Synergetic Antimicrobial Activity Using *Pleurotus ostreatus* Fungus

Ehab B. El Domany[1*], Tamer M. Essam[2], Amr E. Ahmed[1], Ahmed A. Farghali[3]

[1]Biotechnology and Life Sciences Department, Faculty of Postgraduate Studies for Advanced Sciences, Beni-Suef University, Egypt.
[2]Microbiology and Immunology Department, Faculty of Pharmacy, Cairo University, Kasr Al-Aini Street, Cairo 11562, Egypt.
[3]Material Sciences and Nanotechnology Department, Faculty of Postgraduate Studies for Advanced Sciences, Beni-Suef University, Egypt.

ARTICLE INFO

Article history:
Received on: 10/10/2017
Accepted on: 22/03/2018
Available online: 30/05/2018

Key words:
Biosynthesis, Plackett-Burman, gold nanoparticles, anti-cancer, synergic.

ABSTRACT

Biosynthesis of nanoparticles is a valuable method and highly safe with low cost. Gold nanoparticles have an enormous medical application, in recent days. This study demonstrates an optimized biosynthesis for stable gold nanoparticles (AuNPs) using *Pleurotus ostreatus* extracellular filtrate. The biosynthesized gold nanoparticles characterization using UV-Vis spectrophotometer, Zeta seizer, X-ray diffraction, TEM, and FTIR. UV-Vis spectra of gold nanoparticles showed maximum absorption peak at 550 nm. From the TEM images, the size of AuNPs was found to be about 10−30 nm. The physicochemical parameters of gold nanoparticles biosynthesis were studied using Plackett-Burman design. All parameters were highly significant ($p < 0.001$). The rate of AuNPs biosynthesis was found to increase with increasing the salt concentration, incubation time and temperature. On the other hand, lowering both the pH and ratio increase the biosynthesis rate. Furthermore, we compared the anti-proliferation of the biosynthesized and the commercial prepared AuNPs against human liver cancer cell line (HepG2), Prostate cancer cell line (PC3) and Human colon cancer cell line (HCT-116). The biosynthesized AuNPs caused a significant decrease in cell viability of both HepG2 and HCT-116 (33.5%, 22.7%) than commercial AuNPs (29.7%, 9.8%). The synergistic effect of biosynthesized AuNPs gave highest fold increase (11) against *E. coli*, followed by (10) fold against *Staphylococcus auras* using Azithromycin and Amoxicillin as standard antibiotics respectively.

INTRODUCTION

Nanostructures possess valuable and unique chemical, optical and mechanical properties which permit using it in medical therapeutics and diagnosis. Gold nanoparticles (AuNPs) have applications in microbiology, medicine, environmental sensing and biosensors (Kitching *et al.,* 2015). Biosynthesis of AuNPs has more economic advantages than physicochemical methods which need complex and hi-tech instrumentation facilities, harsh chemicals also, biomedical application of Nanoparticles will be safe if these nanoparticles prepared only with biocompatible chemicals to minimize toxicity (Shedbalkar *et al.*, 2014; Mishra *et al.*, 2014). Metal ions have been reduced by the use of bacterial resistance to heavy metal (Gericke and Pinches, 2006). Recently, microorganisms especially bacteria and fungi were shown to be a good alternative to biosynthesize gold nanoparticles (Thakker *et al.*, 2013). However, there is a limited amount of information on the extracellular biosynthesis of gold nanoparticles. Fungi are more realistic than bacteria for production large scale of nanoparticles, including AuNPs biosynthesis due to large secretome include enzymes, active molecules and proteins which play role in capping and reducing AuNPs (Siddiqi and Husen, 2016; Mishra *et al.*, 2014). The growth of fungi is simple in techniques, high yield also easy to extract active components, so it preferred over other organisms in large scale production of nanoparticles (Kumari *et al.,* 2016).

*Corresponding Author
Ehab B. El Domany, Biotechnology and Life Sciences Department, Faculty of Postgraduate Studies for Advanced Sciences, Beni-Suef University, Egypt. E-mail: drehabeldomany @ gmail.com

Physical and biological conditions show significant roles during biosynthesis of nanoparticles. The cell-free extract which contains reducing and capping agent play role in the biosynthesis of nanoparticles. High concentration of proteins can increase the high formation of nanoparticles (Das *et al.,* 2010). AuNPs have Distinct physicochemical properties make them ideal for biomedical applications. Biofunctionalized AuNPs offer many desired Properties for using them as drug carriers as the functionalized AuNPs core is chemically inactive and nontoxic element (Mishra *et al.*, 2014; Patil and Kim, 2016).

Nanomaterials are expected to improve cancer diagnosis and therapy (Rosarin *et al*., 2013). Recently silver and gold nanoparticles used in anticancer therapy for several types of cancer are HepG2 and cell lung cancer cell lines (A549) (Rosarin *et al.*, 2013; Rajeshkumar, 2016). Development effective antimicrobial reagents, free of resistance and cost-effective is an important issue nowadays, due to the prevalence and increase of microorganisms resistant to Majority of antibiotics. Investigation the synergistic effect of biosynthesized AgNPs and AuNPs combined with antibiotics against different types of bacteria and fungi is an important issue in overcome resistance of microorganisms to antibiotics (Fayaz *et al.,* 2010; Prema *et al.*, 2016).

This study aimed to the biosynthesis of AuNPs and optimize the biosynthesis through some factors including pH of medium, Shaking rate, salt concentration, extracellular cell filtrate ratio and temperature of shaker incubator in Biosynthesis process (Bhushan *et al.,* 2014). In this paper, we use Placket-Burman design to optimize AuNPs using response surface resonance to show the effect of tetrachloro auric acid ($HAuCl_4$) conc., pH, agitation, incubation time, temperature, the ratio of Extracellular filtrate (ECF) and $HAuCl_4$ by volume on the quantity of biosynthesized AuNPs. An attempt has been made to obtain a high yield of gold nanoparticles which used in anti-cancer, synergetic antimicrobial activity.

MATERIAL AND METHODS

Culture condition of *Pleurotus ostreatus* fungus

Pleurotus ostreatus fungus was kindly provided by biotechnology center, Faculty of Pharmacy, Cairo University and maintained in slant. The fresh fungus was grown on potato dextrose agar (PDA) and incubated for 7 days at 21°C (Figure 1). In 100 ml distilled water enlymyner flask contain optimized media (Mahfouz *et al.,* 2016) contain 1 gm glucose, 0.5 gm yeast, 0.5 gm malt extract, 0.2 gm KNO_3 at pH 6 then inoculate 3 discsmycelia with diameter 5 mm of fresh fungus and incubate at 30°C for 8 days with shaking 120 rpm. The extracellular fluid was filtrated from biomass using wattman filter paper 0.2 mm then we were measured total protein content using nanodrop (2000) then kept at 2-8c till use.

Biosynthesis and characterization of gold nanoparticles

The cell filtrate was mixed with 2.5 mM $HAuCL_4$ (Sigma Aldrich) in ratio 10:1 for 24 hours at 37c with agitation 120 rpm, the cell filtrate, and the $HAuCL_4$ solution was kept under the same conditions. Changing color from yellow to violet to pink refers to the formation of AuNPs and to confirm that we used UV-visible Spectrophotometer (T80) operated with 1 nm resolution. X-ray Diffraction study was carried out using PANalytical (Empyrean) X-ray diffraction using Cu Kα radiation (wavelength 0.154 cm^{-1}) at an accelerating voltage 40 KV, current of 35 mA, scan angle 5−75° range and scan step 0.02°, AuNPssuspension centrifuged at 10000 rpm for 30 minutes and washed with deionized water twice then ground to fine powder. The dispersed AuNPs were used for FTIR measurement and carried out using Bruker (Vertex 70 FT-IR) spectrometer in the range from 4000 to 400 cm^{-1}. TEM images were obtained by JEOL-JEM 2100 (Japan) with an acceleration voltage of 200 KV, the analysis was prepared by coating aqueous AuNPs drops on the carbon-coated copper grid. Potential and size of AuNPs were measured using Zeta seizer Nano-ZS90 (Malvern, UK) by an applied diluted sample of AuNPs.

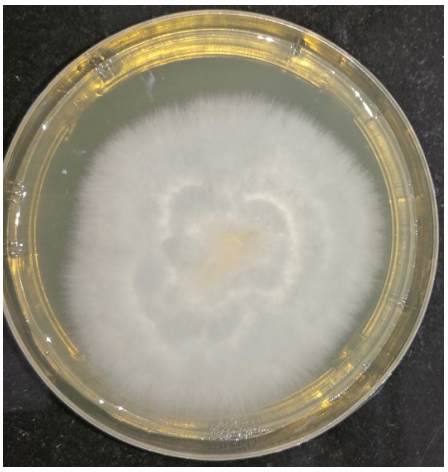

Fig. 1: *P. ostreatus* growth at PDA.

Table 1: Experimental range and levels of independent variables in the Plackett-Burman experiment.

Variables	Levels		
	−1	0	1
pH	5	6	7
Temperature	30	37	40
$HAuCl_4$ Salt conc.	1 mM	2.5 mM	5 mM
Agitation	100 rpm	150 rpm	200 rpm
Time of incubation	12 Hr	24 Hr	48 Hr
Ratio between ECF volume and $HAuCl_4$ salt	5:1	10:1	15:1

Optimization of biosynthesized gold nanoparticles

Placket-Burman experimental design was applied for optimize conditions of Biosynthesis of AuNPs and to show significant factors and their optimum value (Mabrouk and Sabra, 2012; El giddawy *et al.*, 2017). Two level-5 factor experimental blocks were established (Table 1), Six independent factors were included in the studied pH, salt conc., agitation, incubation time, temperature, the ratio between salt and ECF. For each variable, a high (+1) and low (−1) levels were tested and screened in 9 experimental runs (Table 2), where a trial number 9 represented the base condition of biosynthesis before optimization. Triple experiments were done for each run with total 27 runs which were applied according to PB design matrix. The analysis was

calculated using statistical software [MINITAB version (1.0.0.1)] based on fractional factorial design. The response that represents forming AuNPs measuring the intensity of absorbance at 550 nm due to the resonance of gold nanoparticles.

In vitro cell viability and anticancer activity

Cell culture

The study carried out on HepG2, HCT-116, and PC3. Cells were obtained from National Research Centre, Cairo, Egypt and suspended in RPMI 1640 basal medium With L-glutamine and sodium bicarbonate and sterile-filtered (Sigma Aldrich R2405), suitable for the cell. Culturing of cells were done 10 days, then collected at a concentration of 10×10^3 cells/well in fresh complete growth medium in 96-well microtiter plastic plates at 37ºC for 24 h under 5% CO_2 using CO_2 incubator (Sheldon, TC2323, Cornelius, OR, USA). Media has been aspirated then mixed with synthetic AuNPs purchased from (Sigma Aldrich) and biosynthesized AuNPs, Separately. Aspiration of medium occurred After two days of incubation, then we added 40 ul MTT salt (2.5 µg/ml) to each well and incubated for further four hours at 37ºC under 5% CO_2. The reaction was stopped also, dissolving the formed crystals by adding 200 µL of 10% Sodium dodecyl sulphate (SDS) in deionized water to each well and incubated for ten hours at 37ºC. A positive control (100 µg/ml) who gives 100% lethality, was used as a known cytotoxic natural agent under the same conditions (El-Menshawi *et al.,* 2010; Thabrew *et al.*, 1997). The absorbance was then measured using a microplate spectrophotometer (Bio-Rad Laboratories Inc., model 3350, Hercules, California, USA) at 595 nm and a reference wavelength of 620 nm. A statistical significance was tested between samples and negative.

Synergistic effect of AuNPs

The synergistic effect of biosynthesized AuNPs and commercially AuNPs (Sigma Aldrich) was carried out by disc diffusion method. To study the synergistic effect, four standard antibiotic discs as levofloxacin, Azithromycin, Ciprofloxacin and Amoxicillin were impregnated individually with 100 µl each of biosynthesized AuNPs and commercially AuNPs (Figure 2) then, were placed onto the Mueller Hinton Agar medium (0.2 beef extract, 1.75 g casein hydrolysate, 0.15 g starch and 1.7 g agar dissolved in 100 ml H_2O) inoculated with individual test organisms. Standard antibiotic discs alone were used as positive controls. These plates were incubated overnight at 37°C. After incubation, the result was recorded by measuring the inhibitory zone diameter (mm).

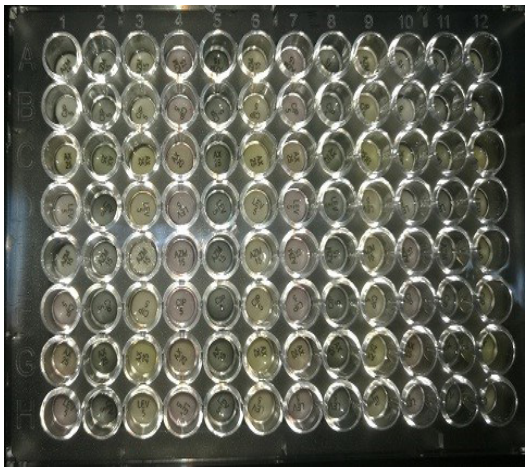

Fig. 2: Different antibiotics with AuNPs.

Table 2: The Plackett-Burman design matrix representing the values of independent factors and the values of measured response.

Run	pH	Temp.	HAuCl4 salt conc.	Agitation	Time of incubation	Ratio	Dummy1	Mean ± SD of absorbance at wave length 550
1	1	1	1	−1	1	−1	−1	1.33 ± 0.14
2	−1	1	1	1	−1	1	−1	0.76 ± 0.01
3	−1	−1	1	1	1	−1	1	1.84 ± 0.01
4	1	−1	−1	1	1	1	−1	0.82 ± 0.01
5	−1	1	−1	−1	1	1	1	0.40 ± 0.01
6	1	−1	1	−1	−1	1	1	0.61 ± 0.04
7	1	1	−1	1	−1	−1	1	0.32 ± 0.05
8	−1	−1	−1	−1	−1	−1	−1	0.45 ± 0.00
9	0	0	0	0	0	0	0	0.62 ± 0.03

RESULTS AND DISCUSSIONS

AuNPs characterization

In this study, stable AuNPs were produced in solution by the extracellular fluid of *Pleurotus ostreatus* fungus. Different intracellular and extracellular methods are used for the production of biological nanoparticles (Prema *et al.*, 2016; Ingle and Rai, 2009). Using nanodrop technique, the total protein content of ECF was 5.404 mg/ml at absorbance 280 wavelength and purity was 1.25 at 260/280 wavelength. Using this ECF, biosynthesis of AuNPs was observed by the change in color from yellow to dark violet color (Figure 3) and characterized by UV-Visible spectroscopy as shown in (Figure 4). Peak around 550 was observed. Gold ions converted to Gold atoms in nano size with changes in color from yellow to violet or red according to reduction size (Zuber *et al.,* 2016; Amendola *et al.*, 2014). This is the characteristic resonance wavelength for the synthesis of AuNPs (Mulvaney, 1996). Prema *et al.* (2016) reported that the maximum absorbance of prepared

AuNPs at 550 nm using *Klebsiella pneumonia* bacteria. The colloidal suspensions of AuNPs were collected then examined by XRD which show crystalline nature of AuNPs (Figure 5). FCC structured of gold show 4 sets of the lattice (111, 200, 220, and 311). These values also reported for gold nanostructures (Du *et al.,* 2007; Deplanche and Macaskie, 2008) an agreement with the database (Wang *et al.*, 1994). The TEM micrographs visualize the size and shape of AuNPs formed (Figure 6a,b) which show that the particles are uneven in a spherical shape with a varying size of 10-30 nm. Similarly, Srinath and Ravishankar (2015) observed that smaller sized AuNPs were almost spherical in shape Zeta seizer and potentially show the good result of dispersion of particles with moderate stability −24MV (Figure 7a,b). FT-IR show band at ~1640 may be the residue of amino acid Capping and stabilizing gold nanoparticles (Figure 8). similarly, Bhat *et al.* (2013) observed Band at 1642 recognized as amide I of biosynthesized gold nanoparticles.

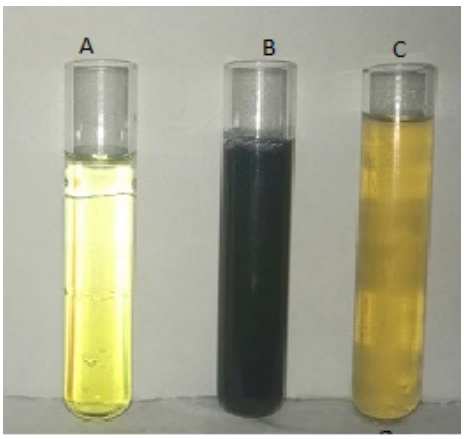

Fig. 3: A) HAuCl4, B) ECF with HAuCl4, C) ECF only.

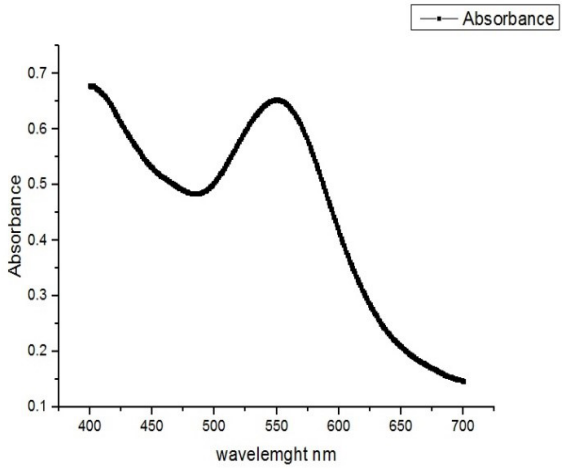

Fig. 4: Absorbance of Gold nanoparticles.

Optimization of biosynthesis conditions

Different physical and biological parameters play role in the production of gold nanoparticles (Kumari *et al.*, 2016). When the statistically based experimental designs using PB model was applied trial no. 3 (pH 5; Temp 30; $HAuCl_4$ salt concentration 5 mM; agitation 200 rpm; time of incubation 48 h; ratio 5:1) gave the highest response for forming gold nanoparticles Table 2. The all six independent variables were significant (p-value < 0.001) for AuNPs biosynthesis process as shown in (Figure 9).

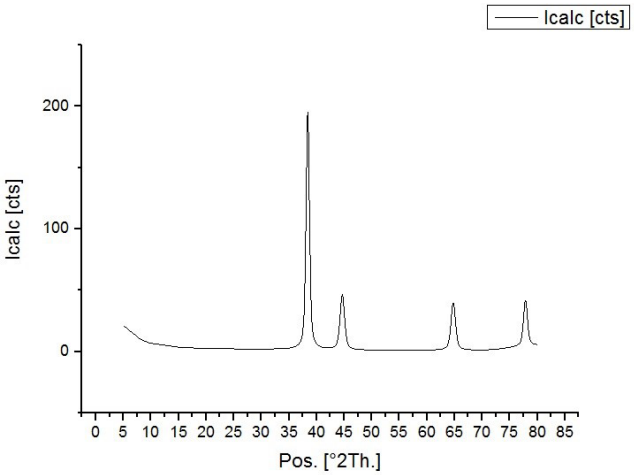

Fig. 5: XRD pattern of gold nanoparticles.

Table 3: Statistical analysis of Plackett-Burman design results showing estimated effect, regression coefficient and corresponding *t*-values, *P*-values and confidence levels for each variable for AuNPs yield.

Term	Effect	Coef	SE Coef	*T*-Value	*P*-Value	VIF
Constant		0.6230	0.0303	20.57	0.000	1.00
pH	−0.0918	−0.0459	0.0107	−4.28	0.000	1.00
Temp.	−0.2269	−0.1135	0.0107	−10.59	0.000	1.00
$HAuCl_4$ Salt conc.	0.6379	0.3190	0.0107	29.78	0.000	1.00
Agitation	0.2389	0.1195	0.0107	11.15	0.000	1.00
Time of incubation	0.5651	0.2825	0.0107	26.38	0.000	1.00
Ratio	−0.3399	−0.1700	0.0107	−15.87	0.000	1.00
Dummy1	−0.0446	−0.0223	0.0107	−2.08	0.052	1.00
pH*Temp.*ratio	−0.3841	−0.1920	0.0321	−5.98	0.000	1.00

The main effects of these variables independently were shown (Figure 10) and their values were presented in (Table 3). $HAuCL_4$ salt concentration was the most effective variable followed by Time of incubation then agitation, they were with positive signs meaning that the higher the value the higher forming gold nanoparticles. Ratio, Temperature, and pH had little effect on forming gold nanoparticles and had negative signs which indicated higher efficiency at lower levels. This was recorded and observed in the three-dimensional surface plot (Figure 11a). The maximum forming AuNPs intensity was achieved when a high value of $HAuCl_4$ salt concentration 10 mM at low ratio 5:1 (Figure 11b). The intensity of absorbance at 550 nm was the response of amount of AuNPs formation. Reduction of Au ions became higher with a high amount of salt concentration 5 mM with 48 hours incubation time at 30°C. Shakouri *et al.* (2016) reported that the maximum gold nanoparticles production was at 96 h after incubation between 2.5 mM gold ions at 28°C and *Aspergillus flavus* supernatant.

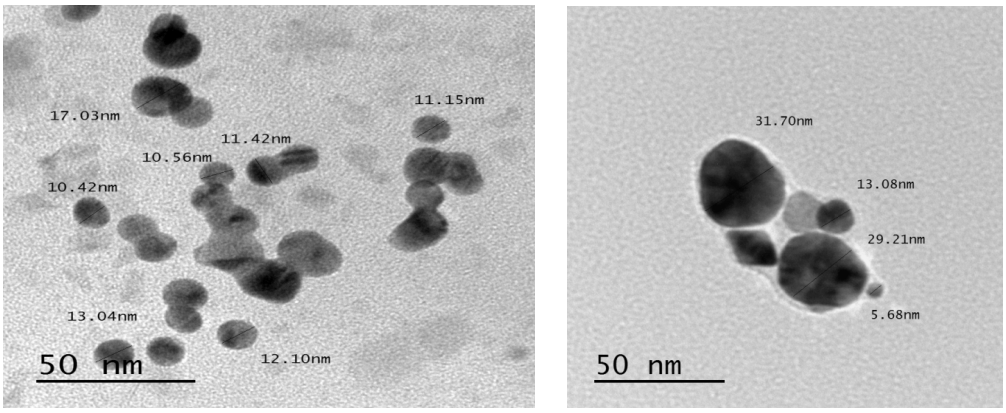

Fig. 6: a) TEM show moderate dispersed of spherical gold nanoparticles. b) TEM show spherical and prism shape gold nanoparticles.

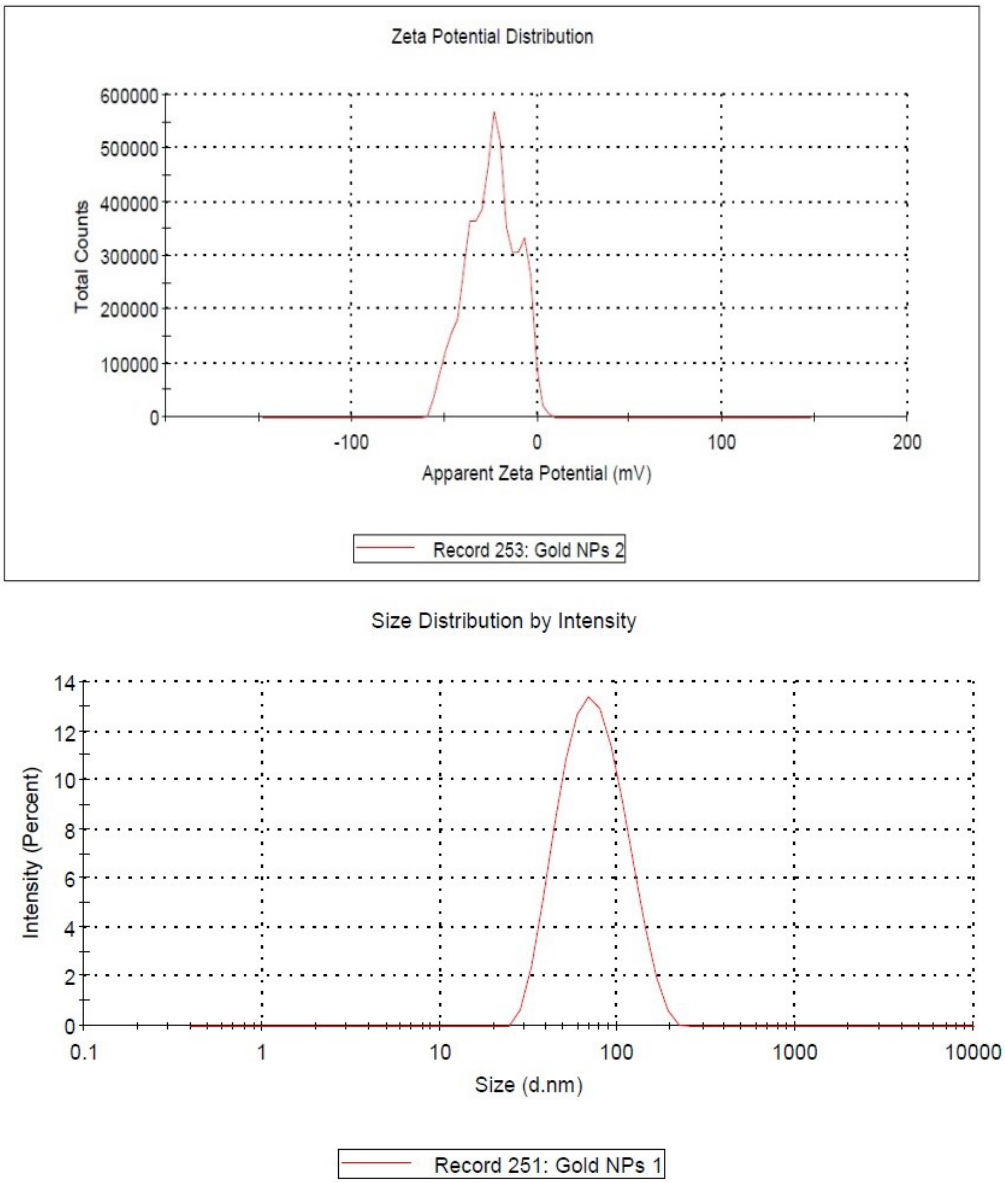

Fig. 7: a) Zeta potential distribution of Gold nanoparticles. b) Size distribution by Gold nanoparticles.

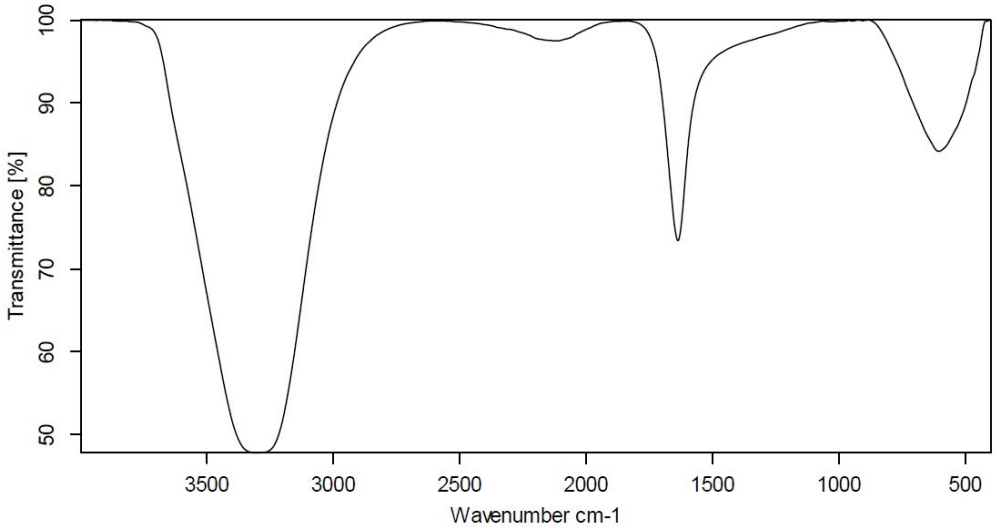

Fig. 8: FTIR of Gold nanoparticles.

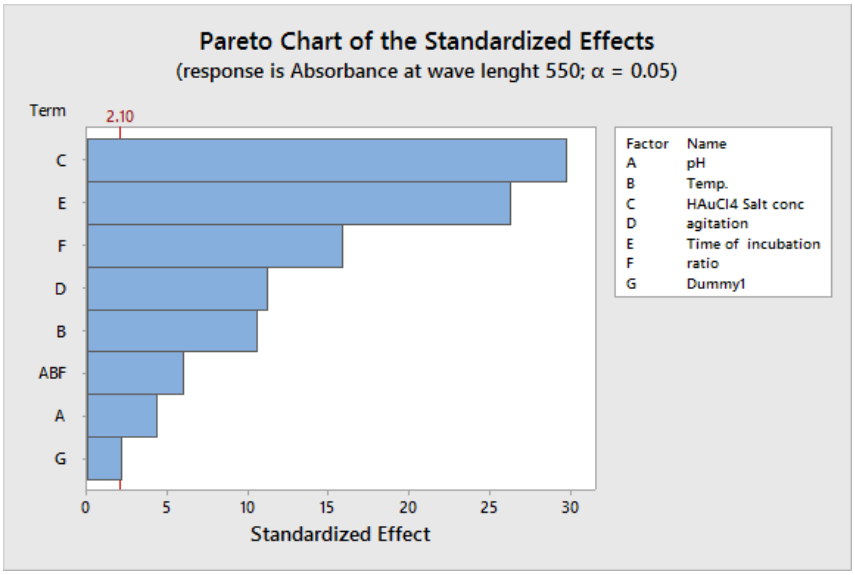

Fig. 9: Standardized effects of all parameters.

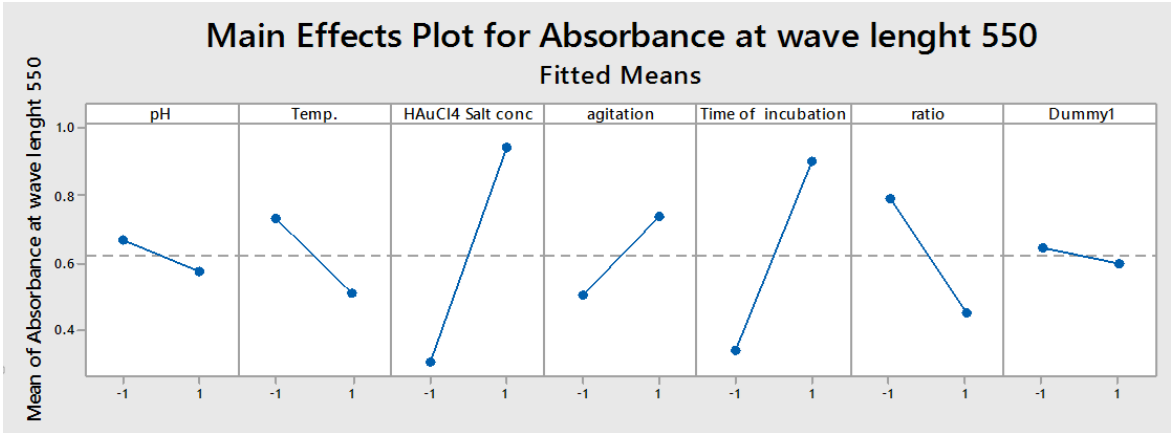

Fig. 10: Main effects of all parameters.

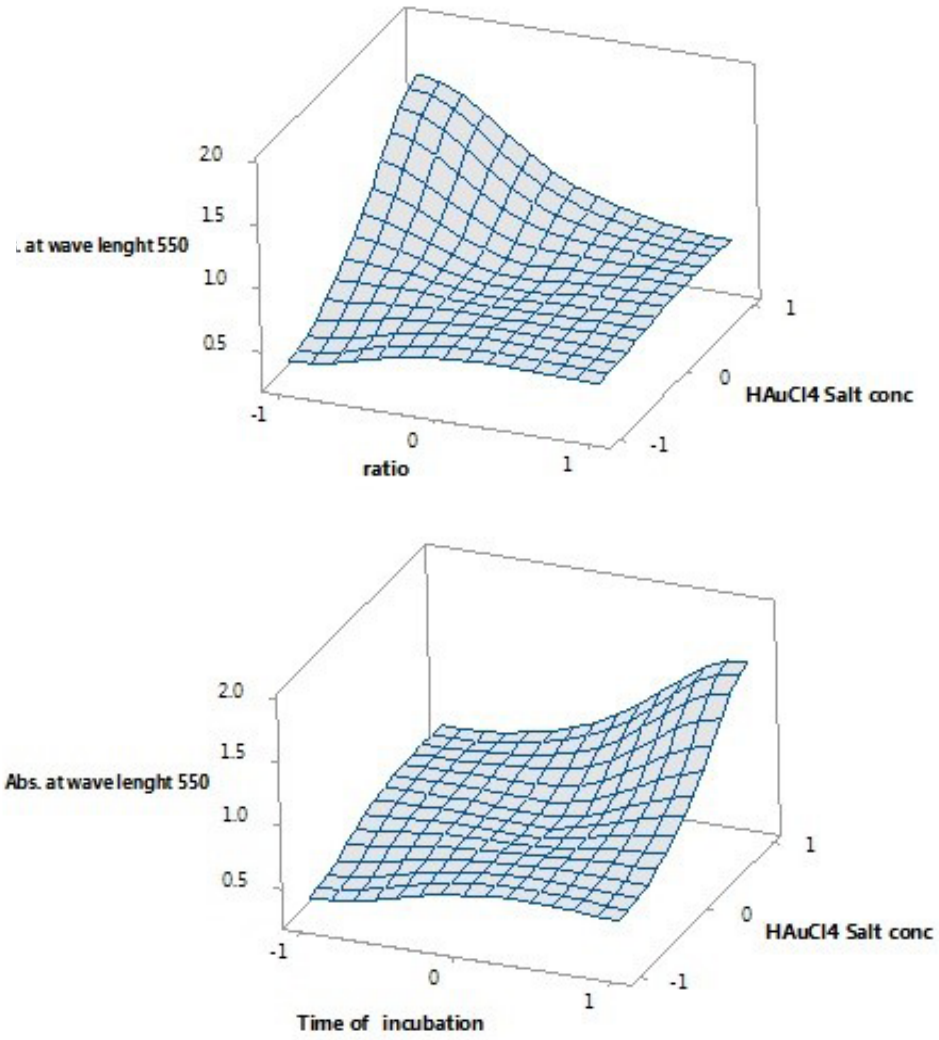

Fig. 11: a) Surface plot of absorbance at wave length 550 vs. HAuCl4 salt conc.; ratio. b) Surface plot of absorbance at wave length 550 vs. HAuCl4 salt conc.; time of incubation.

Anticancer activity

In vitro cytotoxic activity HepG2, HCT-116 and PC3 cell line at biosynthesized AuNPs (25 µg/ml) concentration was evaluated and compared with Commercial purchased AuNPs (25 µg/ml). The anticancer activity of biosynthesized AuNPs against HepG2 and HCT-116 increased more than commercial AuNPs (Figure 12). Further, the most apparent and noticeable effect following treatments of cells to biosynthesized AuNPs is the alteration in the cell shape or morphology of the cells. Concentration 25 µg/ml of biosynthesized AuNPs showed good anticancer activity against HepG2, HCT-116, and PC3 (33.5%, 22.7%, and 14.6%), Sequentially. Bhat *et al.* (2013) showed that AuNPs exhibited positive anti-proliferative activity against different cancer cell lines at 30 µg/ml. The positive results of AuNPs are attributed to their irregular shape and its functionalization with organic moieties (Lee *et al.,* 2015). While comparing the effect of Au nanoparticles on cell viability, Biosynthesized AuNPs show higher proliferation inhibition than commercially AuNPs against HepG2 and HCT-116 but lower against PC3. In fact, Biosynthesized AuNPs is safer in a medical application, the most noticeable effect following treatments of cells to biosynthesized AuNPs is the changing in the morphology of the cells.

The synergetic effect of Gold nanoparticles

The result of the synergistic effect of biosynthesized AuNPs is given in Table 4. It revealed that the distinct difference was observed between the inhibitory zones by antibiotics with and without AuNPs, similarly, Gold and silver nanoparticles showed a synergistic effect against different pathogenic bacteria (Prema *et al*., 2016; El Domany *et al.*, 2017). The enhanced zone of inhibition was observed and it was increased from 25 to 36 mm when the biosynthesized AuNPs were loaded with Azithromycin antibiotics against *E. coli* (Figure 13). Biosynthesized AuNPs enhance the antimicrobial activity of all antibiotics greater than commercial AuNPs with range 1-2 mm in inhibition zone against all tested microorganisms

(Figure 14), so biosynthesized AuNPs are more effective a low-cost preparation and biocompatible because it capped by proteins and other functionalized particles which improve anti-cancer and synergetic antimicrobial activity.

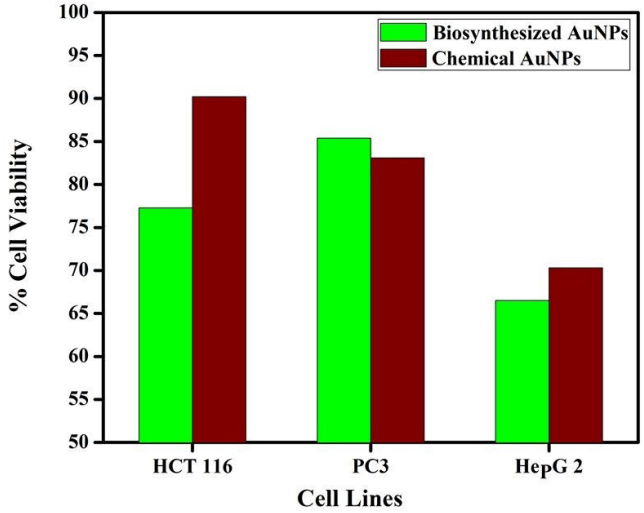

Fig. 12: Effect of biosynthesized and chemically AuNPs on percentage cell viability of HepG2, PC3, and HCT 116 cell lines.

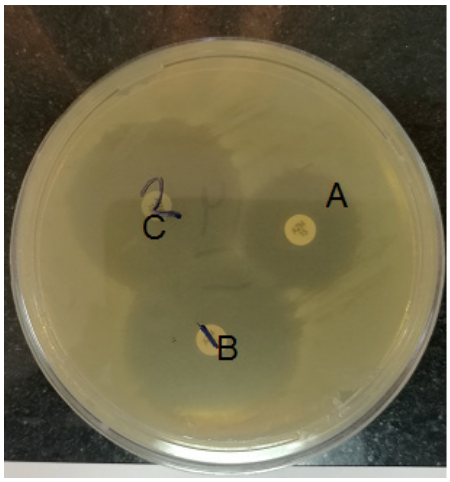

Fig. 13: (A-azithromycin only B-biosynthesized AuNPs with azithromycin C-commercially AuNPs with azithromycin) against *E. coli*.

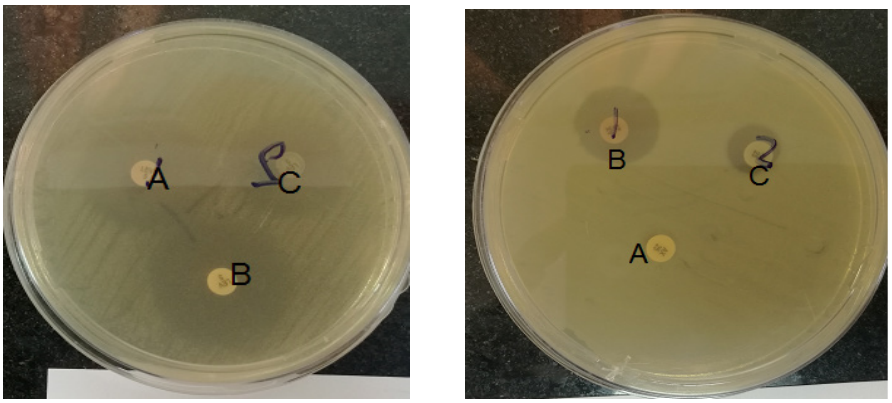

Fig. 14: (1) (A-Levofloxacin only B-Biosynthesized AuNPs with Levofloxacin C-commercially AuNPs with Levofloxacin) against *S. aurus*. (2) (A-Amoxicillin only B-Biosynthesized AuNPs with Amoxicillin C-commercially AuNPs with Amoxicillin) against *E. coli*.

Table 4: Synergistic effect of antibiotics only and combination with biosynthesized AuNPs or commercially AuNPs against the selected human bacterial pathogen.

Pathogens	Antibiotics (µg/disc)	Zone of inhibition (mm) disk only	Zone of inhibition (mm) + biosynthesized AuNPs	Increased zone size (mm)	Zone of inhibition (mm) + commercially AuNPs	Increased zone size (mm)
Bacillus subtilis	Levofloxacin (5 µg)	28	30	2	29	1
	Azithromycin (15 µg)	27	28	1	27	0
	Ciprofloxacin (5 µg)	26	28	2	27	1
	Amoxicillin (25 µg)	18	20	2	19	1
Staph. aurus	Levofloxacin (5 µg)	25	30	5	30	5
	Azithromycin (15 µg)	26	28	2	27	1
	Ciprofloxacin (5 µg)	25	29	4	28	3
	Amoxicillin (25 µg)	17	27	10	25	8
E. coli	Levofloxacin (5 µg)	36	39	3	37	2
	Azithromycin (15 µg)	25	36	11	35	10
	Ciprofloxacin (5 µg)	38	38	0	36	−2
	Amoxicillin (25 µg)	17	18	1	18	1
Candida albican	Levofloxacin (5 µg)	0	13	13	12	12
	Azithromycin (15 µg)	0	11	11	11	11
	Ciprofloxacin (5 µg)	0	12	12	11	11
	Amoxicillin (25 µg)	0	13	13	12	12

CONCLUSION

AuNPs were successfully biosynthesized using edible mushroom *Pleurotus ostreatus* extracellular filtrate as a reducing and capping agents. AuNPs have been characterized by UV-Vis spectroscopy, XRD, TEM, and FTIR. The obtained results confirmed the crystalline nature of AuNPs and morphological studies showed spherical shape of AuNPs with size ranging from 10-30 nm. Zeta potential −24.0 mV for AuNPs reveal moderate stability. Optimization of the chemical and physical parameters achieved to obtain a high yield of gold nanoparticles. Further, biosynthesized AuNPs enhanced anticancer and synergist antimicrobial activity than the commercial AuNPs.

ACKNOWLEDGMENT

This work was supported by Research Development Unit (RDU) at Beni-Suef University (BSU), Egypt.

CONFLICT OF INTEREST

The authors declare that there is no conflict of interest.

REFERENCES

Amendola V, Meneghetti M, Stener M, Guo Y, Chen S, Crespo P, García MA, Hernando A, Pengo P, Pasquato L. Physico-Chemical Characteristics of Gold Nanoparticles. Comprehensive Analytical Chemistry, 2014; 66:81-152.

Bhat R, Sharanabasava VG, Deshpande R, Shetti U, Sanjeev G, Venkataraman A. Photo-biosynthesis of irregular shaped functionalized gold nanoparticles using edible mushroom Pleurotus Florida and its anticancer evaluation. Journal of Photochemistry and Photobiology B: Biology, 2013; 125:63-69.

Bhushan B, Luo D, Schricker SR, Sigmund W, Zauscher S. 2014. Handbook of nanomaterials properties, Springer Science & Business Media.

Das SK, Das AR, Guha AK. Microbial synthesis of multishaped gold nanostructures. Small, 2010; 6(9):1012-1021.

Deplanche K, Macaskie LE. Biorecovery of gold by *Escherichia coli* and Desulfovibrio desulfuricans. Biotechnology and bioengineering, 2008; 99(5):1055-1064.

Du L, Jiang H, Liu X, Wang E. Biosynthesis of gold nanoparticles assisted by *Escherichia coli* DH5α and its application on direct electrochemistry of hemoglobin. Electrochemistry Communications, 2007; 9(5):1165-1170.

El-Menshawi BS, Fayad W, Mahmoud K, El-Hallouty SM, El-Manawaty M, Olofsson MH, Linder S. Screening of natural products for therapeutic activity against solid tumors. Indian Journal of Experimental Biology, 2010; 48(3):258-264.

El Domany EB, Essam TM, Ahmed AE, Farghali AA. Biosynthesis, Characterization, Antibacterial and Synergistic Effect of Silver Nanoparticles using Fusarium oxysporum. Journal of Pure and Applied Microbiology, 2017; 11(3):1441-1446.

El giddawy N, Essam TM, Rouby WM, Raslan M, Farghali AA. New approach for enhancing Chlorella vulgaris biomass recovery using ZnAl-layered double hydroxide nanosheets. Journal of Applied Phycology, 2017. New approach for enhancing Chlorella vulgaris biomass recovery using ZnAl-layered double hydroxide nanosheets. Journal of Applied Phycology, 2017; 29:1399-1407.

Fayaz AM, Balaji K, Girilal M, Yadav R, Kalaichelvan PT, Venketesan R. Biogenic synthesis of silver nanoparticles and their synergistic effect with antibiotics: a study against gram-positive and gram-negative bacteria. Nanomedicine, 2010; 6(1):103-9.

Gericke M, Pinches A. Microbial production of gold nanoparticles. Gold Bulletin, 2006; 39(1):22-28.

Ingle A, Rai M, Gade A, Bawaskar M. Fusarium solani: a novel biological agent for the extracellular synthesis of silver nanoparticles. Journal of Nanoparticle Research, 2009; 11:2079-2085.

Kitching M, Ramani M, Marsili E. Fungal biosynthesis of gold nanoparticles: mechanism and scale up. Microbial biotechnology, 2015; 8(6):904-917.

Kumari M, Mishra A, Pandey S, Singh SP, Chaudhry V, Mudiam MK, Shukla S, Kakkar P, Nautiyal CS. Physico-chemical condition optimization during biosynthesis lead to development of improved and catalytically efficient gold nano particles. Scientific reports, 2016; 8(6):27575.

Lee KD, Nagajyothi PC, Sreekanth TVM, Park S. Eco-friendly synthesis of gold nanoparticles (AuNPs) using *Inonotus obliquus* and their antibacterial, antioxidant and cytotoxic activities. Journal of Industrial and Engineering Chemistry, 2015; 26:67-72.

Mabrouk M, Abou-Zeid D, Sabra W. Application of Plackett-Burman experimental design to evaluate nutritional requirements for poly (γ-glutamic acid) production in batch fermentation by Bacillus licheniformis A13. Afr. J. Appl. Microbiol. Res, 2012; 1:6-18.

Mahfouz AM, Essam TM, Amin MA. Enhancement of Microbial Synthesis of Gold Nanoparticles by Gamma Radiation. British Journal of Applied Science & Technology, 2016; 17(4):1-14.

Mishra A, Kumari M, Pandey S, Chaudhry V, Gupta KC, Nautiyal CS. Biocatalytic and antimicrobial activities of gold nanoparticles synthesized by *Trichoderma* sp. Bioresource technology, 2014; 166:235-242.

Mulvaney P. Surface plasmon spectroscopy of nanosized metal particles. Langmuir, 1996; 12(3):788-800.

Patil MP, Kim GD. Eco-friendly approach for nanoparticles synthesis and mechanism behind antibacterial activity of silver and anticancer activity of gold nanoparticles. Applied Microbiology and Biotechnology, 2017; 101(1):79-92.

Prema P, Iniya PA, Immanuel G. Microbial mediated synthesis, characterization, antibacterial and synergistic effect of gold nanoparticles using Klebsiella pneumoniae (MTCC-4030). RSC Advances, 2016; 6(6):4601-4607.

Srinath BS, Ravishankar RV. Biosynthesis of highly monodispersed, spherical gold nanoparticles of size 4–10 nm from spent cultures of Klebsiella pneumoniae. 3 Biotech, 2015; 5(5):671-676.

Rajeshkumar S. Anticancer activity of eco-friendly gold nanoparticles against lung and liver cancer cells. Journal of Genetic Engineering and Biotechnology, 2016; 14(1):195-202.

Rosarin FS, Arulmozhi V, Nagarajan S, Mirunalini S. Antiproliferative effect of silver nanoparticles synthesized using amla on Hep2 cell line. Asian Pacific journal of tropical medicine, 2013; 6(1):1-10.

Shakouri V, Salouti M, Mohammadi B, Zonooz NF. Procedure optimization for increasing biosynthesis rate of gold nanoparticles by Aspergillus flavus Supernatant. Synthesis and Reactivity in Inorganic, Metal-Organic, and Nano-Metal Chemistry, 2016; 46(10):1468-1472.

Shedbalkar U, Singh R, Wadhwani S, Gaidhani S, Chopade BA. Microbial synthesis of gold nanoparticles: Current status and future prospects. Advances in colloid and interface science, 2014; 209:40-48.

Siddiqi KS, Husen A. Fabrication of Metal Nanoparticles from Fungi and Metal Salts: Scope and Application. Nanoscale research letters, 2016; 11(1): 98.

Thabrew M, Hughes RD, Mcfarlane IG. Screening of hepatoprotective plant components using a HepG2 cell cytotoxicity assay. Journal of pharmacy and pharmacology, 1997; 49(11):1132-1135.

Thakker JN, Dalwadi P, Dhandhukia PC. Biosynthesis of gold nanoparticles using Fusarium oxysporum f. sp. cubense JT1, a plant pathogenic fungus. ISRN biotechnology, 2013; 2013, Article ID 515091, 5 pages.

Wang A, Han J, Guo L, Yu J, Zeng P, Wang A. Database of standard Raman spectra of minerals and related inorganic crystals. Applied Spectroscopy, 1994; 48(8):959-968.

Zuber A, Purdey M, Schartner E, Forbes C, van der Hoek B, Giles D, Ebendorff-Heidepriem H. Sensors and Actuators B: Chemical Detection of gold nanoparticles with different sizes using absorption and fluorescence based method. Sensors and Actuators B: Chemical, 2016; 227:117-127.

How to cite this article:
El Domany EB, Essam TM, Ahmed AE, Farghali A.A. Biosynthesis Physico-Chemical Optimization of Gold Nanoparticles as anti-cancer and synergetic antimicrobial activity using *Pleurotus ostreatus* fungus. J App Pharm Sci, 2018; 8(05): 119-128.